Catal Lett (2009) 129:163–169
DOI 10.1007/s10562-008-9784-y

Production of Middle Distillate Through Hydrocracking of Paraffin Wax over NiMo/SiO_2–Al_2O_3 Catalysts: Effect of SiO_2–Al_2O_3 Composition on Acid Property and Catalytic Performance of NiMo/SiO_2–Al_2O_3 Catalysts

Sunhwan Hwang · Joohyung Lee · Sunyoung Park · Dong Ryul Park · Ji Chul Jung · Sang-Bong Lee · In Kyu Song

Received: 11 November 2008 / Accepted: 13 November 2008 / Published online: 13 December 2008

Abstract SiO_2–Al_2O_3 supports with different composition were prepared by a precipitation method in order to control the acid property of SiO_2–Al_2O_3 supports. NiMo/SiO_2–Al_2O_3 catalysts were then prepared by an impregnation method and sulfided for use in the production of middle distillate through hydrocracking of paraffin wax. It was revealed that MoS_2 phase was dominantly formed in the NiMo/SiO_2–Al_2O_3 catalysts, while Ni–Mo–S phase was not detected due to its fine dispersion. Acidity of NiMo/SiO_2–Al_2O_3 catalysts measured by NH_3–TPD experiments showed a volcano-shaped curve with respect to SiO_2 content. Acidity of the catalysts played an important role in determining the catalytic performance in the hydrocracking of paraffin wax. Conversion of paraffin wax was monotonically increased with increasing acidity of the catalyst, while yield for middle distillate showed a volcano-shaped curve with respect to acidity of the catalyst. Thus, optimal acidity of NiMo/SiO_2–Al_2O_3 catalysts was required for the maximum production of middle distillate through hydrocracking of paraffin wax.

Keywords Hydrocracking · Paraffin wax · NiMo/SiO_2–Al_2O_3 · Middle distillate

S. Hwang · J. Lee · S. Park · D. R. Park · J. C. Jung · I. K. Song (✉)
School of Chemical and Biological Engineering, Institute of Chemical Processes, Seoul National University, Shinlim-dong, Kwanak-ku, Seoul 151-744, South Korea
e-mail: inksong@snu.ac.kr

S.-B. Lee
Korea Research Institute of Chemical Technology, Daejeon 305-600, South Korea

1 Introduction

Hydrocracking is a key process in petroleum refining for the conversion of heavy hydrocarbons into a variety of high-value fuels such as gasoline (C_5–C_{11}) and middle distillate (C_{10}–C_{20}) [1–3]. In particular, hydrocracking process is of great importance to meet the growing demand for high-quality middle distillate requiring stringent specifications [4]. Although crude oil has been traditionally used as a heavy hydrocarbon source for the production of middle distillate [5], Fischer–Tropsch (F–T) wax has also attracted much attention as an alternate feed for the production of middle distillate [6]. F–T wax is typically composed of *n*-paraffins (>90%), alcohols, and olefins. An important feature of F–T wax is that it is virtually free of sulfur (<5 ppm) and contains extremely low aromatic compounds (<1%). Furthermore, middle distillate produced from F–T wax retains high cetane number (ca. 70), which is significantly higher than the minimum required value for conventional diesel (ca. 51). Therefore, production of middle distillate through hydrocracking of F–T wax has been recognized as an economical and environmentally benign process.

Hydrocracking is generally conducted over metal/acid bifunctional catalysts [7–11]. Alkanes are dehydrogenated on the metallic sites and then isomerized or cracked on the acid sites through classical and non-classical carbenium ion chemistry [12–14]. The most conventional hydrocracking catalysts used for the production of gasoline or diesel from crude oil are NiMo and NiW catalysts supported on alumina [15], silica–alumina [16], fluorine-doped alumina [17], USY zeolite [18], and molecular sieves [19]. Pd or Pt-loaded solid acid catalysts have also been investigated for the hydrocracking of heavy hydrocarbons [20]. Although Ni–Mo/silica–alumina catalyst has been employed for upgrading crude oil [21], no noticeable progress has been

made on the production of middle distillate through hydrocracking of F–T wax (*n*-paraffin) over NiMo/silica–alumina catalyst.

In this work, a series of SiO_2–Al_2O_3 supports with different composition were prepared by a precipitation method, with an aim of controlling the acid property of SiO_2–Al_2O_3 supports. NiMo/SiO_2–Al_2O_3 catalysts were then prepared by an impregnation method and sulfided for use in the production of middle distillate through hydrocracking of paraffin wax. NH_3–TPD experiments were conducted to investigate the effect of support composition on acid property of NiMo/SiO_2–Al_2O_3 catalysts. The acid property of NiMo/SiO_2–Al_2O_3 catalysts was then correlated with their catalytic performance in the hydrocracking of paraffin wax.

2 Experimental

2.1 Preparation of NiMo/SiO_2–Al_2O_3 Catalysts

SiO_2–Al_2O_3 supports with different composition were prepared by a precipitation method. Known amount of Al precursor ($AlCl_3 \cdot 6H_2O$, Fluka) was dissolved in 200 mL of distilled water, and pH of the solution was adjusted at 7.0 using ammonia solution. After maintaining the solution for 1 h at 55 °C, known amount of Si precursor (tetraethyl orthosilicate, TEOS, Sigma–Aldrich) was added into the solution containing Al precursor. The resulting solution was then aged for 40 min at pH = 8.0. After recovering solid by filtration, the solid was washed with distilled water several times. The solid was dried in a convection oven at 110 °C for 10 h, and then it was calcined at 550 °C for 3 h to obtain a SiO_2–Al_2O_3 support. The composition of SiO_2–Al_2O_3 supports was controlled by changing the amounts of Al and Si precursors. The prepared SiO_2–Al_2O_3 supports with different composition were denoted as SA(28), SA(52), SA(68), SA(74), and SA(88). Here, the number in parenthesis represents the weight percentage of SiO_2 in the SiO_2–Al_2O_3 support.

NiMo catalysts supported on SiO_2–Al_2O_3 were prepared by an impregnation method using a mixed aqueous solution containing ammonium molybdate tetrahydrate ($(NH_4)_6Mo_7O \cdot 4H_2O$, Samchun) and nickel nitrate hexahydrate ($Ni(NO_3)_2 \cdot 6H_2O$, Fluka). In all the supported catalysts, NiO and MoO_3 loadings were adjusted at ca. 5 and ca. 20 wt%, respectively. After drying the impregnated catalysts overnight at 110 °C, they were calcined at 500 °C for 3 h. The prepared catalysts were denoted as NiMo/SA(28), NiMo/SA(52), NiMo/SA(68), NiMo/SA(74), and NiMo/SA(88). Each NiMo/SiO_2–Al_2O_3 catalyst was sulfided in a tubular fixed-bed reactor by flowing a mixed stream (34,283 mL/h g) of H_2S (10%) and H_2 (90%) at 360 °C for 3 h under atmosphere pressure, prior to use in NH_3–TPD (temperature-programmed desorption) measurement and catalytic reaction.

2.2 Characterization of NiMo/SiO_2–Al_2O_3 Catalysts

Composition of NiO, MoO_3, SiO_2, and Al_2O_3 in the supported catalyst was determined by ICP–AES measurement (Shimadz, ICP-1000IV). Sulfur content in the sulfided catalyst was measured by CHNS elemental analysis (Leco, CHNS-932). Surface area and pore volume of the catalyst were measured using a BET apparatus (Micromeritics, ASAP 2010). Crystalline phase of the catalyst was investigated by XRD measurement (MAC Science, M18XHF-SRA) using Cu-Kα radiation ($\lambda = 1.54056$ Å) operated at 50 kV and 200 mA.

NH_3–TPD experiment was conducted to determine the acid property of sulfided catalyst. A volume of 0.1 g of NiMo/SiO_2–Al_2O_3 catalyst was charged into a quartz reactor of the TPD apparatus, and then it was pretreated at 200 °C for 1 h with a stream of helium (20 mL/min). After cooling the catalyst to room temperature, NH_3 (20 mL) was pulsed into the reactor every minute under a flow of helium (5 mL/min) until the acid sites were saturated with NH_3. After evacuating the catalyst sample at 50 °C for 1 h, the catalyst was further treated with a stream of helium (15 mL/min) to remove physisorbed NH_3. The furnace temperature was then increased from room temperature to 800 °C at a heating rate of 10 °C/min under a flow of helium (10 mL/min). The desorbed NH_3 was detected using a GC–MSD (Agilent, MSD-6890 N).

2.3 Hydrocracking of Paraffin Wax

Figure 1 shows the schematic diagram of reaction system. Hydrocracking of paraffin wax to produce middle distillate was carried out over sulfided NiMo/SiO_2–Al_2O_3 catalyst in a stainless steel autoclave reactor (75 mL). A volume of 0.7 g of sulfided catalyst and 18 g of paraffin wax

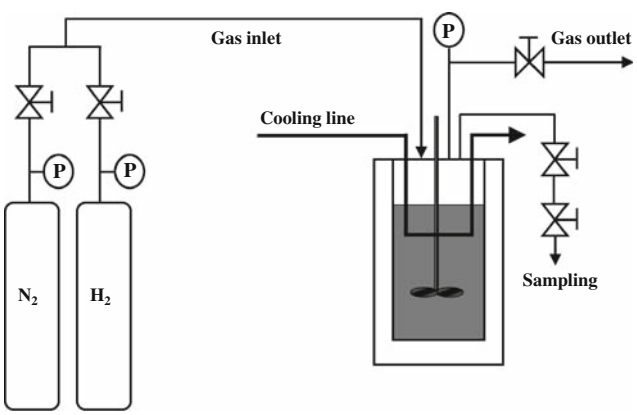

Fig. 1 Schematic diagram for reaction system

Table 1 Carbon number distribution of paraffin wax

Carbon number	21	22	23	24	25	26	27	28	29	30	31	32	33	34
wt%	0.4	1	2.8	5.5	9.1	11.3	11.8	10.9	9.7	8.7	10.4	10.3	7.8	0.3

(Sigma–Aldrich) were placed in the autoclave reactor at room temperature. After purging the reactor with N_2 several times, the reactor was pressurized to 35 bar with H_2. The reactor was then heated to reaction temperature (400 °C). The catalytic reaction was carried out for 2 h at H_2 pressure of 60 bar. After the reaction, the reactor was cooled to room temperature and the products were collected for analysis. The products were analyzed with gas chromatographs (Younglin 600D and Younglin ACME 6100). For comparison and reference, the reaction was also conducted in the absence of catalyst. Carbon number distribution of paraffin wax (melting point: 58–62 °C, ASTM D87) was in the range of C_{21}–C_{34} (Table 1). Wax conversion and product selectivity were calculated according to the Eqs. (1)–(4). Yield for middle distillate (C_{10}–C_{20}) was calculated by multiplying conversion of wax and selectivity for middle distillate.

3 Results and Discussion

3.1 Characterization Results of NiMo/SiO_2–Al_2O_3 Catalysts

Chemical composition, BET surface area, and pore volume of NiMo/SiO_2–Al_2O_3 catalysts are summarized in Table 2. NiO and MoO_3 compositions in the supported catalysts were in the range of 4.6–5.0 and 18.8–21.6 wt%, respectively. These values were in good agreement with the designed values, indicating that all the supported catalysts were successfully prepared as attempted in this work. SiO_2 content in the NiMo/SiO_2–Al_2O_3 catalysts was intentionally controlled to be distributed within the wide range of 28–88 wt%, in order to investigate the effect of support composition on acid property and catalytic performance of NiMo/SiO_2–Al_2O_3 catalysts. BET surface area of the

$$\text{Wax } (C_{21+}) \text{ conversion } (\%) = \frac{\text{wt\% of } C_{21+} \text{ in the feed} - \text{wt\% of } C_{21+} \text{ in the product}}{\text{wt\% of } C_{21+} \text{ in the feed}} \times 100 \quad (1)$$

$$C_1-C_4 \text{ selectivity } (\%) = \frac{\text{wt\% of } C_1-C_4 \text{ in the product}}{\text{wt\% of } C_{21+} \text{ in the feed} - \text{wt\% of } C_{21+} \text{ in the product}} \times 100 \quad (2)$$

$$C_5-C_9 \text{ selectivity } (\%) = \frac{\text{wt\% of } C_5-C_9 \text{ in the product}}{\text{wt\% of } C_{21+} \text{ in the feed} - \text{wt\% of } C_{21+} \text{ in the product}} \times 100 \quad (3)$$

$$C_{10}-C_{20} \text{ (middle distillate) selectivity } (\%) = \frac{\text{wt\% of } C_{10}-C_{20} \text{ in the product}}{\text{wt\% of } C_{21+} \text{ in the feed} - \text{wt\% of } C_{21+} \text{ in the product}} \times 100 \quad (4)$$

Table 2 Characterization results of NiMo/SiO_2–Al_2O_3 catalysts

Catalyst	NiO (wt%)[a]	MoO_3 (wt%)[a]	SiO_2 (wt%)[a]	BET surface area (m^2/g)	Pore volume (cm^3/g)[b]	Sulfur content (wt%)[c]
NiMo/SA(28)	4.7	20	28	262	0.53	10.2
NiMo/SA(52)	4.6	20	52	204	0.69	9.3
NiMo/SA(68)	4.6	20	68	202	0.77	9.1
NiMo/SA(74)	5.0	18.8	74	200	0.82	9.1
NiMo/SA(88)	4.8	21.6	88	85	0.28	9.0

[a] Determined by ICP–AES measurement

[b] Calculated by BJH model

[c] Measured by CHNS elemental analysis after sulfidation

catalysts decreased with increasing SiO_2 content. Pore volume of the catalysts showed a volcano-shaped curve with respect to SiO_2 content. Among the catalysts, NiMo/SA(74) exhibited the largest pore volume. Sulfur content of the catalysts measured after sulfidation showed no great difference with respect to SiO_2 content.

3.2 Crystalline Phases of NiMo/SiO_2–Al_2O_3 Catalysts

Figure 2 shows the XRD patterns of NiMo/SiO_2–Al_2O_3 catalysts calcined at 500 °C. Each crystalline phase was identified using JCPDS. All the calcined catalysts were composed of three major mixed phases of MoO_3, α-$NiMoO_4$, and β-$NiMoO_4$. However, XRD peaks for NiO were not observed in all the catalysts. This means that NiO particles were finely dispersed on the SiO_2–Al_2O_3 supports, resulting in the formation of small NiO particles that were under detection limit of XRD measurement. It is noticeable that XRD peak intensities for MoO_3 and $NiMoO_4$ increased with increasing SiO_2 content. This is because SiO_2 retains weaker metal-support interaction than Al_2O_3 [22].

Figure 3 shows the XRD patterns of NiMo/SiO_2–Al_2O_3 catalysts sulfided at 360 °C. MoS_2 phase was gradually developed and became strong with increasing SiO_2 content. However, Ni–Mo–S phase was not detected in all the catalysts. This result also means that Ni–Mo–S particles were finely dispersed on the SiO_2–Al_2O_3 supports by forming small Ni–Mo–S particles that were under detection limit of XRD measurement [23], as observed for NiO particles (Fig. 2). It was also reveled that Ni_3S_4, NiS, and Ni_3S_2 phases were not detected in all the sulfided NiMo/SiO_2–Al_2O_3 catalysts.

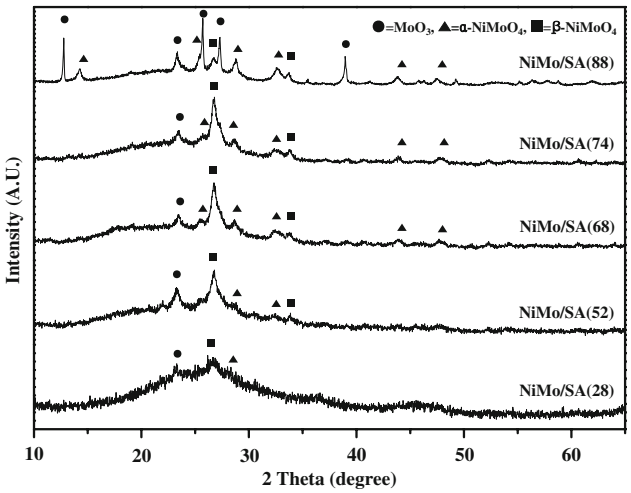

Fig. 2 XRD patterns of NiMo/SiO_2–Al_2O_3 catalysts calcined at 500 °C

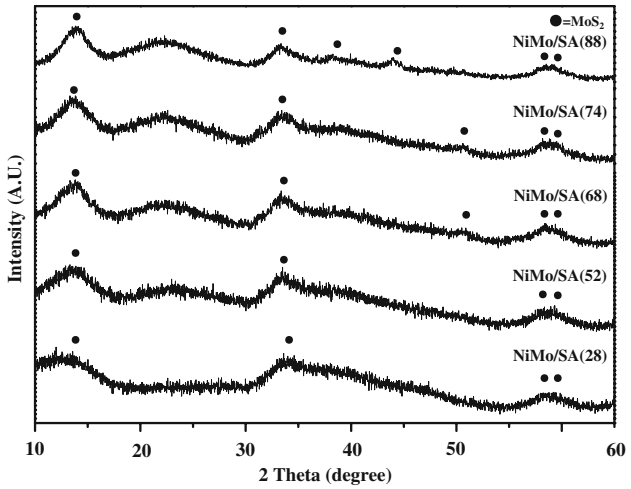

Fig. 3 XRD patterns of NiMo/SiO_2–Al_2O_3 catalysts sulfided at 360 °C

3.3 Acidity of NiMo/SiO_2–Al_2O_3 Catalysts

Figure 4 shows the NH_3–TPD profiles of selected NiMo/SiO_2–Al_2O_3 catalysts sulfided at 360 °C. NiMo/SiO_2–Al_2O_3 catalysts showed a major desorption peak at around 200 °C with no great difference and an additional minor desorption peak (shoulder) at around 400 °C. Acidities of sulfided NiMo/SiO_2–Al_2O_3 catalysts are summarized in Table 3. Acidity of the catalysts showed a volcano-shaped curve with respect to SiO_2 content. Among the catalysts tested, NiMo/SA(52) exhibited the largest acidity.

3.4 Hydrocracking of Paraffin Wax over NiMo/SiO_2–Al_2O_3 Catalysts

Performance of NiMo/SiO_2–Al_2O_3 catalysts for hydrocracking of paraffin wax performed at 400 °C and 60 bar for 2 h is listed in Table 4. In the absence of catalyst,

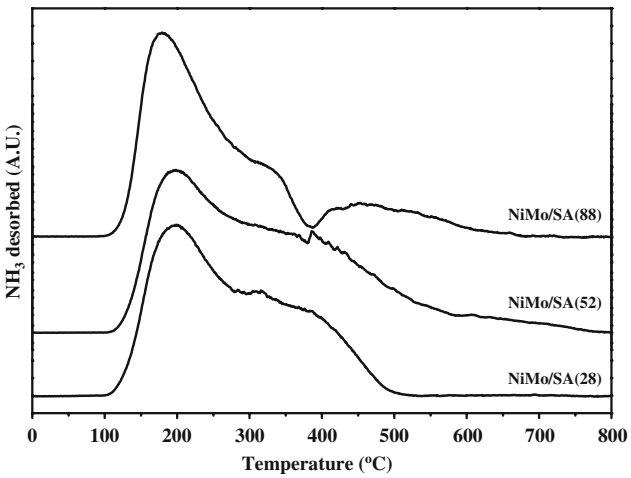

Fig. 4 NH_3–TPD profiles of selected NiMo/SiO_2–Al_2O_3 catalysts sulfided at 360 °C

Table 3 Acidity of sulfided NiMo/SiO_2–Al_2O_3 catalysts

Catalyst	Acidity (mmol-NH_3/g-catalyst)
NiMo/SA(28)	0.135
NiMo/SA(52)	0.164
NiMo/SA(68)	0.148
NiMo/SA(74)	0.147
NiMo/SA(88)	0.129

conversion of wax was very low although selectivity for middle distillate was high, resulting in low yield for middle distillate. This result indicates that mild hydrocracking of paraffin wax occurred in the absence of catalyst. All the NiMo/SiO_2–Al_2O_3 catalysts showed an enhanced conversion of wax and comparable selectivity for middle distillate compared to the case of no catalyst. As a consequence, yield for middle distillate (target product) in the presence of NiMo/SiO_2–Al_2O_3 catalysts was much higher than that in the absence of catalyst. In other words, NiMo/SiO_2–Al_2O_3 catalysts were very efficient for the production of middle distillate through hydrocracking of paraffin wax. Among the catalysts tested, NiMo/SA(68) showed the highest yield for middle distillate.

Figure 5 shows the carbon number distributions of paraffin wax (reactant) and product over NiMo/SA(52) catalyst. The result clearly shows that much portion of paraffin wax was hydrocracked to light hydrocarbons including middle distillate. This result also supports that NiMo/SiO_2–Al_2O_3 catalysts were suitable for hydrocracking of paraffin wax to middle distillate.

3.5 Correlation Between Acidity and Catalytic Performance of NiMo/SiO_2–Al_2O_3 Catalysts

Figure 6 shows the correlation between acidity and conversion of wax over NiMo/SiO_2–Al_2O_3 catalysts. Conversion of paraffin wax was monotonically increased with increasing acidity of the catalyst. This can be understood by the fact that hydrocracking ability of the catalyst increased

Table 4 Performance of NiMo/SiO_2–Al_2O_3 catalysts for hydrocracking of paraffin wax

	Wax conversion (%)	Product selectivity (%)			C_{10}–C_{20} yield (%)
		C_1–C_4	C_5–C_9	C_{10}–C_{20}	
No catalyst	11.0	21.1	30.5	48.4	5.3
NiMo/SA(28)	33.9	19.7	30.8	49.5	16.8
NiMo/SA (52)	75.4	19.0	50.9	30.1	22.7
NiMo/SA(68)	64.6	16.8	44.8	38.4	24.8
NiMo/SA(74)	62.9	19.7	45.3	35.0	22.0
NiMo/SA(88)	33.3	20.2	41.0	38.8	12.9

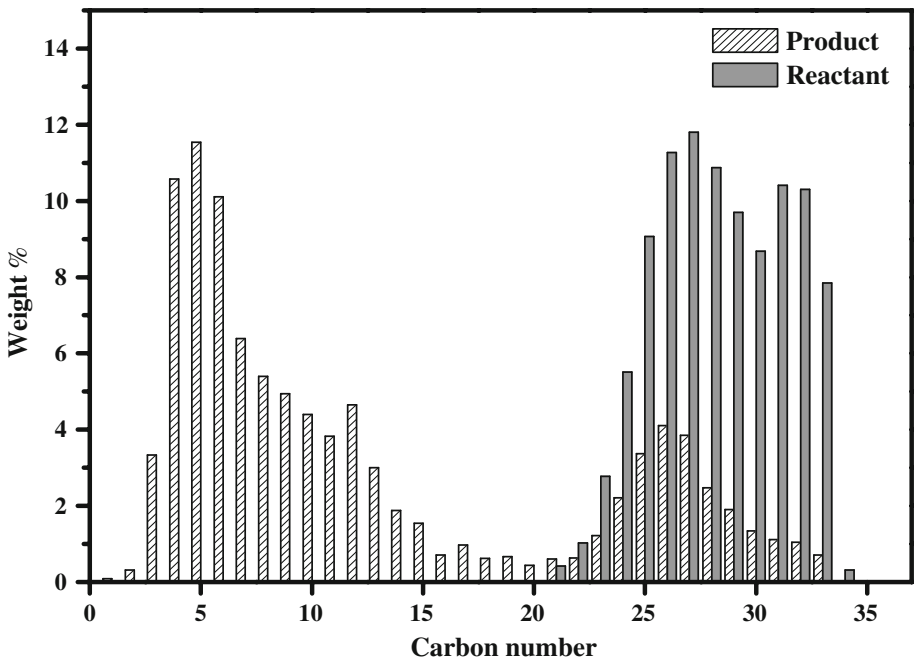

Fig. 5 Carbon number distributions of paraffin wax (reactant) and product over NiMo/SA(52) catalyst

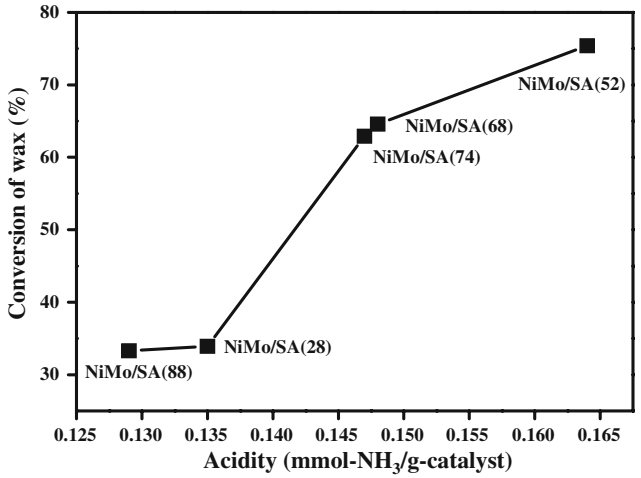

Fig. 6 Correlation between acidity and conversion of wax over $NiMo/SiO_2–Al_2O_3$ catalysts. Acidity and conversion of wax were taken from Tables 3 and 4, respectively

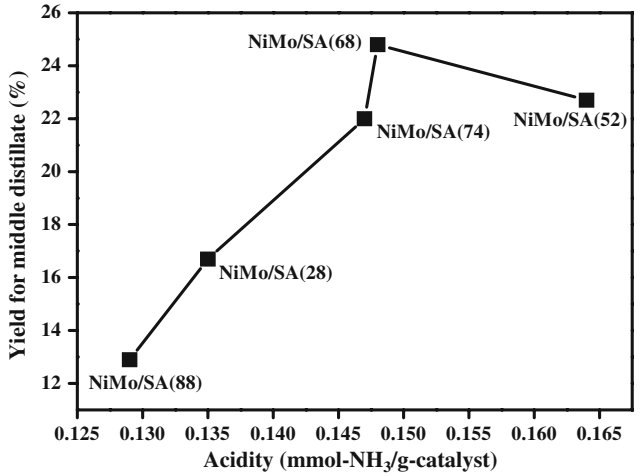

Fig. 7 Correlation between acidity and yield for middle distillate over $NiMo/SiO_2–Al_2O_3$ catalysts. Acidity and yield for middle distillate were taken from Tables 3 and 4, respectively

with increasing acid property of the catalyst [24]. An attempt has been made to correlate acid strength with conversion of wax. However, no reliable correlation between acid strength and conversion of wax was observed. The above result indicates that acidity rather than acid strength played a crucial role in determining the catalytic performance of $NiMo/SiO_2–Al_2O_3$ catalysts in the hydrocracking of paraffin wax.

Figure 7 shows the correlation between acidity and yield for middle distillate over $NiMo/SiO_2–Al_2O_3$ catalysts. It should be noted that yield for middle distillate showed a volcano-shaped curve with respect to acidity of the catalyst. Among the catalysts tested, NiMo/SA(68) retaining moderate acidity showed the highest yield for middle distillate. This result indicates that optimal acidity of $NiMo/SiO_2–Al_2O_3$ catalysts was required for the maximum production of middle distillate through hydrocracking of paraffin wax. In other words, a $NiMo/SiO_2–Al_2O_3$ catalyst with small acidity yields low conversion of wax, while a $NiMo/SiO_2–Al_2O_3$ catalyst with large acidity causes deep hydrocracking of paraffin wax to undesired light hydrocarbon product.

4 Conclusions

A series of $SiO_2–Al_2O_3$ supports with different composition were prepared by a precipitation method, with an aim of controlling the acid property of $SiO_2–Al_2O_3$ supports. $NiMo/SiO_2–Al_2O_3$ catalysts prepared by an impregnation method were then sulfided for use in the production of middle distillate through hydrocracking of paraffin wax. NH_3–TPD experiments were conducted to measure the acid property of $NiMo/SiO_2–Al_2O_3$ catalysts. BET surface area and pore volume of $NiMo/SiO_2–Al_2O_3$ catalysts strongly depended on the SiO_2 content. MoS_2 phase was dominantly formed in the sulfided $NiMo/SiO_2–Al_2O_3$ catalysts, while Ni–Mo–S phase was not detected in the catalysts due to its fine dispersion. Acidity of $NiMo/SiO_2–Al_2O_3$ catalysts showed a volcano-shaped curve with respect to SiO_2 content. It was revealed that acidity of the catalysts served as a crucial factor determining the catalytic performance of $NiMo/SiO_2–Al_2O_3$ catalysts in the hydrocracking of paraffin wax. Conversion of paraffin wax was increased with increasing acidity of the catalyst, while yield for middle distillate showed a volcano-shaped curve with respect to acidity of the catalyst. Among the catalysts tested, NiMo/SA(68) retaining moderate acidity showed the highest yield for middle distillate. It is concluded that optimal acidity of $NiMo/SiO_2–Al_2O_3$ catalysts was required for the maximum production of middle distillate through hydrocracking of paraffin wax.

Acknowledgments The authors would like to acknowledge funding from the Korea Ministry of Knowledge Economy (MKE) through "Energy Technology Innovation Program".

References

1. Ming L, Ji-qian W, Wen-an D, Guo-he Q (2007) J Fuel Chem Technol 35:558–562
2. Pellegrini L, Bonomi S, Gamba S, Calemma V, Molinari D (2007) Chem Eng Sci 62:5013–5020
3. Ali MA, Tatsumi T, Masuda T (2002) Appl Catal A Gen 233: 77–90
4. Alsobaai AM, Zakaria R, Hameed BH (2007) Fuel Process Technol 88:921–928
5. Yang H, Fairbridge C, Hill J, Ring Z (2004) Catal Today 93–95:457–465
6. Cho KM, Park S, Seo JG, Youn MH, Baeck S-H, Jun K-W, Chung JS, Song IK (2008) Appl Catal B Environ 83:195–201

7. Robinson WRAM, van Veen JAR, de Beer VHJ, van Santen RA (1999) Fuel Process Technol 61:89–101
8. Robinson WRAM, van Veen JAR, de Beer VHJ, van Santen RA (1999) Fuel Process Technol 61:103–116
9. Fujikawa T, Idei K, Ebihara T, Mizuguchi H, Usui K (2000) Appl Catal A Gen 192:253–261
10. Ancheyta-Juárez J, Aguilar-Rodríguez E, Salazar-Sotelo D, Marroquín-Sáncheza G, Quiroz-Sosa G, Leiva-Nuncio M (1999) Appl Catal A Gen 183:265–272
11. Benazzi E, Leite L, Marchal-George N, Toulhoat H, Raybaud P (2003) J Catal 217:376–387
12. Rezgui Y, Guemini M (2005) Appl Catal A Gen 282:45–53
13. Fang K, Wei W, Ren J, Sun Y (2004) Catal Lett 93:235–242
14. Mohanty S, Kunzru D, Saraf DN (1990) Fuel 69:1467–1473
15. Morawski I, Mosio-Mosiewski J (2006) Fuel Process Technol 87:659–669
16. Rezgui Y, Guemini M (2005) Appl Catal A Gen 282:45–53
17. Benitez A, Ramirez J, Cruz-Reyes J, López AA (1997) J Catal 172:137–145
18. Alsobaai AM, Zakaria R, Hameed BH (2007) Chem Eng J 132:77–83
19. Egia B, Cambra JF, Arias PL, Güemez MB, Legarreta JA, Pawelec B, Fierro JLG (1998) Appl Catal A Gen 169:37–53
20. Calemma V, Peratello S, Perego C (2000) Appl Catal A Gen 190:207–218
21. Sánchez-Minero F, Ramírez J, Gutiérrez-Alejandre G, Fernández-Vargas C, Torres-Mancera P, Cuevas-Garcia R (2008) Catal Today 133–135:267–276
22. Rana MS, Maity SK, Ancheyta J, Dhar GM, Prasada Rao TSR (2003) Appl Catal A Gen 253:165–176
23. Yoosuk B, Kim JH, Song C, Ngamcharussrivichai C, Prasassarakich P (2008) Catal Today 130:14–23
24. Alsobaai AM, Zakaria R, Hameed BH (2007) Chem Eng J 132:173–181